JOURNAL OF PROPULSION AND POWER
Vol. 17, No. 5, September–October 2001

Effect of Ambient Pressure on an Airblast Spray Injected into a Crossflow

May Y. Leong,* Vincent G. McDonell,† and G. Scott Samuelsen‡
University of California, UCI Combustion Laboratory, Irvine, California 92697-3550

The injection of a fuel spray into a cross stream was studied for its application in rapid fuel–air mixing for lean combustion processes. The fuel is injected as either a discrete stream or as a partially to fully atomized jet of droplets. Of particular interest was the penetration of the outer and inner edges of the spray of liquid fuel into the gaseous airstream. The experiment focused on exploring the effect of flow conditions on the spray surface trajectories from the point of injection to a downstream distance of $z/D_{\text{fuel}} = 35$. Tests were conducted under ambient pressures of 1, 3, and 5 atm at atomizing air pressure drops varying from 0 to 4.8% for a jet-A fuel flow of 0.18 g/s and a baseline crossflow air velocity of 38 m/s. A modified definition of the jet-to-crossflow momentum-flux ratio q_2 was developed to accommodate a two-phase jet and was subsequently used to obtain a relationship between the flow conditions and the spray surface trajectories. The effect of the degree of atomization in the spray resulting from the change in operating conditions was incorporated by implementing a pressure ratio correction factor into the correlating equation.

Nomenclature

A_{airbl}	=	area associated with the airblast air, assumed as the difference between A_{spray} and A_{liquid}
A_{liquid}	=	area associated with the fuel injection orifice
A_{spray}	=	area associated with the spray injection orifice
C_d	=	orifice discharge coefficient
c_n	=	correlation constants, $n = 0, 1, 2, 3$
D_{fuel}	=	fuel injection orifice diameter
D_{spray}	=	spray injection orifice diameter
q_1	=	single-phase jet-to-crossflow momentum-flux ratio
q_2	=	two-phase jet-to-crossflow momentum-flux ratio
V	=	velocity
We_{cross}	=	crossflow-associated Weber number $\rho_{\text{air}} V_{\text{cross}}^2 D_{\text{fuel}}/\sigma$
x	=	penetration distance
z	=	downstream distance
ρ	=	density

Introduction

TO meet increasingly stringent emissions regulations, combustors for the next generation of advanced gas turbine engines are being designed to reduce pollutant formation while maintaining efficient performance. These combustors may operate under fuel-lean conditions to avoid the high temperatures that are associated with stoichiometric combustion and that are also conducive to the formation of pollutants such as NO_x. Operating the combustor under fuel-lean conditions may still result in high rates of pollutant production if the fuel and air are not thoroughly mixed in both spatial[1,2] and temporal domains[3] before reaction. In addition, stability needs to be maintained and is generally degraded by improved mixing. Hence, the dispersion of liquid fuel into air must be optimized to maintain stability while minimizing pollutant formation.

A simple method of fuel injection involves the injection of a liquid jet into a high-velocity crossflow of air. The crossflow induces pressure drag and viscous drag forces on the jet, leading to the primary breakup of the jet through the fracture of as well as stripping at the surface of the jet column. The residual ligaments and drops produced by primary atomization then undergo secondary breakup by the crossflow until a critical Weber number is attained. The injection of pure liquid jets into a crossflow has been the subject of numerous studies[4–20] that have characterized jet breakup,[4,8,10–13,16,17,19] penetration,[4–6,15,19] and the resultant distributions of mass flux, droplet size, and droplet velocity[7–9,14,16–18,20] of the atomized liquid jet.

One particular fuel injection technique being considered in future low-NO_x combustion strategies involves the injection of a fuel spray into a cross stream of high-velocity air. The spray jet in this study differs from the liquid jet in that it is composed of atomized liquid particles in the form of ligaments and droplets. Injecting the fuel as a partially atomized spray reduces the mixing length otherwise needed to break up a pure liquid jet. The jet–crossflow dynamics and interaction, if properly delineated, also offers the potential of adjusting jet penetration and droplet dispersion to provide optimal performance across the entire duty cycle.

The dispersion of spray jets in a crossflow has been investigated in studies geared toward agricultural applications, for which a spray drift in weak crosswind velocities that are typically less than 10 m/s is simulated.[21–24] The spray jets in these studies were produced from flat-fan pressure atomizers. An alternative to using pressure-based atomizers is to use a high-velocity airstream to help induce instabilities leading to the breakup of the liquid jet. In gas turbine combustion, fuel injectors that employ airblast atomization require lower supply pressures to deliver the fuel, while also partially premixing the air and liquid fuel before its mixing with the rest of the airflow for combustion.[25] Plain-jet airblast atomization, combined with the jet-in-crossflow mixing dynamics, offers a simple and practical means of effecting a uniformly and rapidly mixed fuel–air mixture for gas turbine combustion.

A review of the literature yielded few studies related to the airblast-atomized spray jet in a crossflow. Although the dispersion of a particle-laden jet, composed of a gaseous jet loaded with spherical particles, could simulate the spray jet in crossflow system, the studies performed on particle-laden jets[26–28] have primarily been confined to classes of uniformly sized particles. Predictive models have also been applied to determine the trajectory of droplets in different size classes.[29,30] Although they are helpful in determining the penetration of different classes of size particles, the findings in Refs. 26–30 do not incorporate the case of the spray that is not fully atomized as it emerges into the crossflow.

Received 13 September 2000; revision received 24 January 2001; accepted for publication 24 January 2001.

*Graduate Researcher, Combustion Laboratory; currently Associate Research Engineer, Systems Department, United Technologies Research Center. Member AIAA.

†Senior Research Scientist, Combustion Laboratory. Senior Member AIAA.

‡Professor, Combustion Laboratory. Associate Fellow AIAA.

A few studies have been performed on an airblast spray injection experiment in which distributions formed from the dispersion of the airblast-atomized spray jet into a crossflow were characterized. The experiments described in Ref. 31 feature a custom set of hardware that injected an airblast-atomized spray jet from a round orifice into an unconfined, uniform crossflow of air. Tests reported in Refs. 31 and 32 were performed under atmospheric pressure and utilized methanol as the test fluid. Although the results were useful in demonstrating the utility of the experiment and in assessing trends from the parametric tests, the geometric and operating conditions did not approach the practical conditions of an industrial gas turbine combustor. As a step toward bridging these experiments with practical applications, the present study is conducted under elevated pressures, with the use of a distillate fuel as the liquid injectant and with the implementation of a confined crossflow width that corresponds to the gap in an existing fuel injector design.[33] Because the intent of the experiment is to gauge the effect of pressure on the spray jet formation and dispersion, elevated temperatures were not considered to preclude the effect of vaporization on the spray.

The previous tests described in Refs. 31 and 32 focused on characterizing planar distributions of liquid concentration and droplet size and velocities within the spray. However, views of the overall structure and penetration of the spray, obtained through video imaging, can be as effective and also more efficient in screening the performance of a multitude of spray conditions. Whereas the spray can be assessed qualitatively, the extent of its penetration into the crossflow can be quantified by correlations. The penetration of the jet can be described by the loci of a maximum measured quantity, such as velocity and temperature for a gaseous jet,[34] or volume flux for a liquid jet.[20] Liquid jet penetration has also been quantified by considering their outer surface penetration.[19] In this experiment, the penetration of the spray jets is characterized by quantifying the outer and inner trajectories of the spray surface.

The objectives of this study were to conduct screening tests of a plain-jet, airblast spray jet-in-crossflow injector at conditions that approach geometric and operating conditions that are more applicable to gas turbine engines, and to use the results to develop correlations that describe the outer and inner boundaries of the spray. Such equations can be used as a design tool for engineers to determine the tendency of the spray toward over- and underpenetration, as well as to describe the extent that the spray spreads across the crossflow.

Experiment

Hardware and Facilities

The hardware used in this experiment (see Fig. 1) is the same as that designed and tested in Ref. 31. However, modifications made to the hardware, which included shortening the fuel tube and integrating a traversing system, facilitated the installation of the experiment into the elevated pressure facility. Care was taken to ensure that these modifications did not impact the spray behavior compared to the previous hardware. Additional modifications to the injection panel facilitated the interchanging of parts to vary the geometric configuration, but the changes did not affect the internal flow path of the injector or the spray behavior. The experiment is oriented for spray injection in the $+x$ direction and a cross-stream airflow along the $+z$ direction. The origin is concentric with the orifices of the fuel injector and the spray injection panel.

The hardware primarily consists of the crossflow-conditioning section and the spray injection panel. The crossflow-conditioning section is designed to transition the airflow from a 152.4-mm-diam circular pipe to a rectangular cross section measuring 18.0 by 76.2 mm, with the former value representing the maximum allowable penetration distance of the spray jet. Although the study in Ref. 31 utilized a wider cross section of 101.6 mm, the 18.0-mm transverse width of the present study corresponds to the gap in the mixing section of the fuel injector used in a lean-burn combustion strategy.[33]

The rectangular duct that confined the crossflow comprised the spray injection panel, an opposing stainless steel panel, and two side quartz window panes through which the spray was measured. The geometry of the spray injection panel (see Fig. 1) was also based on the dimensions of the lean-burn fuel injector described in Ref. 33. A stream of liquid fuel emerges from the fuel injector tip through a hole of diameter $D_{\text{fuel}} = 0.34$ mm. The tip of the fuel injector protrudes 1.59 mm from the back face of the spray injection panel, which corresponds to a distance that is one-half of the total atomizing air channel width. Air is supplied to the channel (of length times width times depth of $92.7 \times 19.1 \times 3.18$ mm) such that the air impinges on

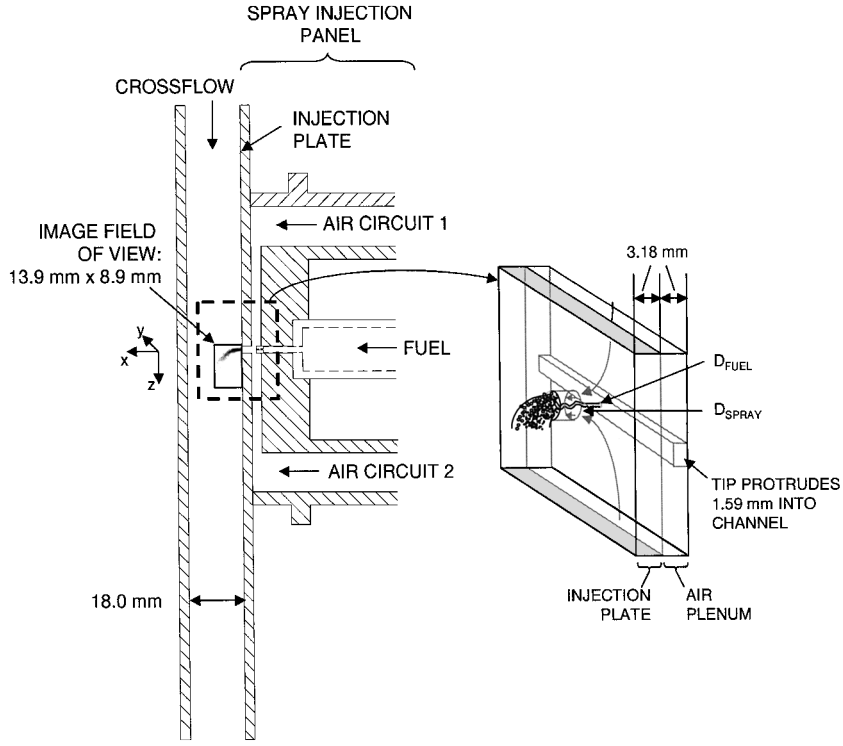

Fig. 1 Details of the airblast spray jet injector hardware.

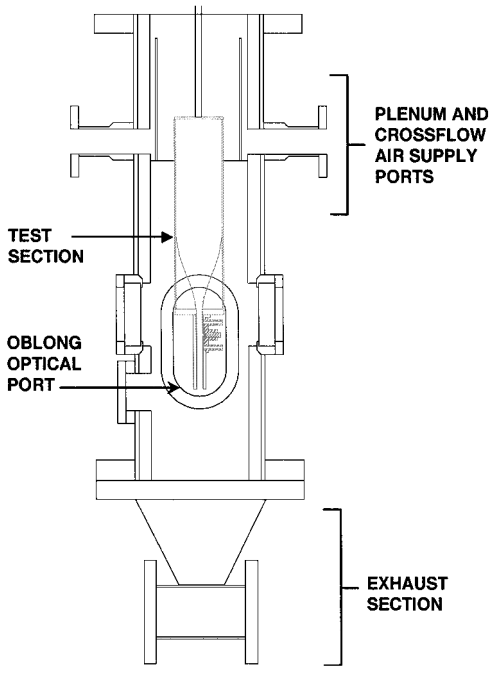

Fig. 2 Airblast spray jet injection hardware installed in the elevated pressure facility.

the liquid fuel from opposing directions. The atomized liquid and air mixture emerges from the 3.18 mm-thick injection plate into the crossflow through a spray orifice diameter of $D_{\text{spray}} = 2.26$ mm. The discharge coefficient C_d of the spray orifice was 0.63.

To vary the ambient pressure in the tests, the hardware was installed in the elevated pressure facility (see Fig. 2). The pressure vessel is rated for operation of up to 15 atm and provides optical access to the spray through ports containing 44.5-mm-thick oblong Pyrex windows.

Conditions

The experiment was operated under ambient pressures of 1, 3, and 5 atm (1.0, 3.1, and 5.2 bars). The fuel and air temperatures initially entered the test section at 20°C. The airblast airflow rate is adjusted to yield various atomizing air-to-liquid mass flow ratios (ALR) that produce different pressure drops across the injection orifice. The corresponding airblast pressure drops varied from 0 to 4.8% of the ambient pressure in the vessel. The mass flow rate of the liquid fuel, jet-A (Unocal), is maintained at a constant mass flow rate of 0.18 g/s. Whereas temperature is not a variable in this experiment, the ambient pressures, fuel flow, and atomizing and crossflow airflows correspond to a low-power operating regime in practical engine applications.

Although the baseline crossflow velocity magnitude was set at 38 m/s, the crossflow was also set at two other velocities at the airblast $\Delta P = 2\%$ setting: 46 and 54 m/s for the 1- and 3-atm cases and 31 and 46 m/s for the 5-atm case. The 5-atm case used a lower set of crossflow velocities to avoid jet attachment to the near wall of the injection panel. Laser anemometry (phase Doppler particle analyzer, Aerometrics transmitter Model 1100-3S and receiver Model 2100-3) was used to measure the uniformity of the crossflow velocity profile at 5 atm. Alumina particles (Microgrit WCA, size 3, microabrasives) of a size range between 2.85 and 3.71 μm, yielding Stokes numbers less than 1 for the range of crossflow velocities tested, were seeded into the crossflow of air to measure the velocity profile. The transverse and axial velocity components of these particles were obtained across a grid of points located at a plane above the orifice at $z = -5$ mm. The grid of points was limited in scope by the potential clipping of either the laser beams from the transmitter or the collection cone of the receiver. As a result, the grid was confined to a cross section limited to $-30 < y < 30$ mm, and $2 < x < 15$ mm. Spatial deviations of the axial velocity over this region were found to be within 2% of the mean value. The maximum turbulent fluctuation of the axial component was 10%. With regard to the other velocity components, the transverse (x direction) velocity component was within 4% of the mean axial component, whereas the y-directional component of the crossflow velocity was assumed negligible. Overall, the measurements indicated that the crossflow velocity primarily comprised the axial velocity component and was uniform in both magnitude and direction.

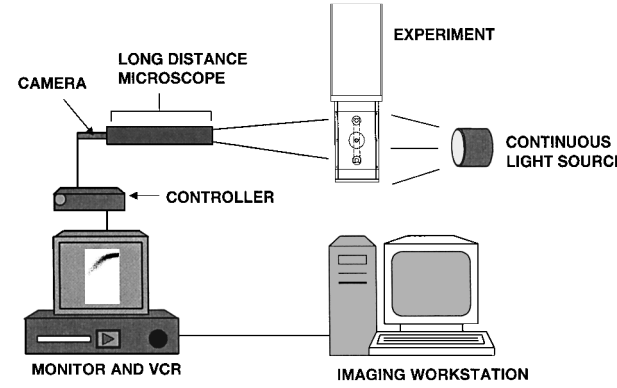

Fig. 3 Video imaging train to capture spray scattering.

Diagnostic

High-magnification video (Fig. 3) characterized the global behavior of the sprays for a wide range of conditions. A 60-W incandescent flood lamp housed in a reflective dome illuminated the spray from the rear. A charge-coupled device video camera (Toshiba 1KM41A) attached to a long distance microscope lens (Infinity Model KV) captured a field of view measuring 13.9 × 8.9 mm, with an image resolution of 29.6 pixels/mm. A 30-s segment of video was recorded using a video cassette recorder (Sony SVO-2000). A computer acquired images from the video and returned a 15-frame-averaged image that was processed to reduce background noise.

For each frame-averaged image, the spray outer and inner surface trajectories were mapped to clarify the extent that the spray penetrated into the crossflow. The spray boundary was denoted by pixel intensity values greater than a threshold level of 30 (out of a maximum intensity level of 255), which was the minimum value that distinguished the shape of the spray.

Momentum-Flux Ratio of the Two-Phase Jet in Crossflow

To compare results from the various test combinations of ALR, crossflow velocity, and ambient pressure, a nondimensional parameter was sought to cast the flow conditions on a common basis. For a jet in a crossflow, an important flow parameter that determines jet penetration is the jet-to-crossflow momentum-flux ratio.[35] For a single-phase jet, the momentum-flux ratio q is simply defined as

$$q = q_1 = (\rho V^2)_{\text{jet}} \big/ (\rho V^2)_{\text{cross}} \tag{1}$$

where the jet refers to either gaseous or liquid phase and the subscript for q refers to the number of phases of the jet. Although the present definition of q suitably defines single-phase jets, this definition does not represent very well a two-phase jet such as that encountered in the present experiment. Because the penetration of the jet into the crossflow depends primarily on q, a similar parameter was developed to produce correlations describing the airblast spray penetration into the crossflow.

For this study, a composite definition of the two-phase jet momentum flux is obtained to represent the numerator of Eq. (1). Given negligible fuel vaporization, as well as negligible kinetic energy losses, the exiting momentum of the spray on leaving the injection plate is presumed to be equal to the initial momentum of both fluids before their entering the control volume (see the control volume in Fig. 4). The total momentum entering the control volume is given by

$$\text{spray jet momentum} = \rho_{\text{liquid}} V_{\text{liquid}}^2 A_{\text{liquid}} + \rho_{\text{air}} V_{\text{airbl}}^2 A_{\text{airbl}} \tag{2}$$

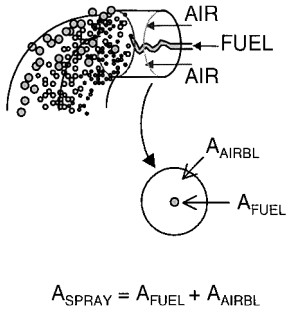

Fig. 4 Control volume used in defining two-phase jet-to-crossflow momentum-flux ratio q_2.

where A_{liquid} refers to the area associated with the fuel injection orifice and A_{airbl} corresponds to the difference between the area of the spray orifice A_{spray} and A_{liquid}.

To obtain the momentum flux of the two-phase jet, the spray jet momentum in Eq. (2) is divided by A_{spray}. The momentum-flux formulation for the two-phase jet q_2 can, thus, be defined as

$$q_2 = \frac{\left[(\rho V^2 A)_{\text{liquid}} + (\rho V^2 A)_{\text{airbl}}\right] / A_{\text{spray}}}{(\rho V^2)_{\text{cross}}} \tag{3}$$

where A_{liquid} refers to the area of the fuel injector hole and A_{airbl} refers to the annular region between the injection panel and fuel injector orifice diameters. The areas in the q_2 expression refer to the geometric areas based on the injector dimensions. The densities of jet-A and air (for both airblast and crossflow air) used in the definition are 819 and 1.19 kg/m^3, respectively. For the different velocities used in Eq. (3), V_{liquid} depends on the metered liquid mass flow rate, the density of jet-A, and A_{liquid}; V_{airbl} is calculated from the pressure drop measurements across the spray orifice; and V_{cross} is derived from the metered crossflow air supply.

In the q_2 expression, the airblast contribution dominates that of the fuel by two to four orders of magnitude. Although the air-to-liquid density ratio is on the order of 10^{-3}, the velocity of the airblast stream is at least 25 times as high as the fuel velocity. When squared, the atomizing air velocity nearly compensates for the low-density factor of the air. In addition, the area associated with the fuel stream is only 2.3% of the area associated with the atomizing air, which further decreases the impact of the fuel momentum contribution to q^2.

Results

Baseline Case: Pure Liquid Jet ($\Delta P_{\text{air}} = 0\%$, ALR = 0)

A baseline comparison of a pure liquid jet injected into a crossflow at the different ambient pressure conditions is presented in Fig. 5. Time-averaged images of the spray are shown on a normalized intensity scale with white corresponding to 0 and black corresponding to 1. The spray is captured with the spray injected from the right side of the image. The left edge of the image corresponds approximately to the midpoint of the crossflow channel, as depicted in Fig. 1. For each image, the single-phase jet to crossflow momentum-flux ratio q_1 and the Weber number We_{cross}, based on the crossflow air velocity are noted. For comparison, the two-phase jet-to-crossflow momentum-flux ratio q_2 is also presented. Note that the q_2 values are lower because they differ from q_1 by a factor of $A_{\text{liquid}}/A_{\text{spray}}$. In addition, We_{cross} is noted because the crossflow contributes primarily to the aerodynamic breakup of the liquid jet.

In the 1-atm case, the outer and inner surfaces of the jet are distinct. However, in the 3- and 5-atm cases, the inner spray surface is not distinctly seen because the spray attaches to the near wall. As the ambient pressure increases, the crossflow air density increases. This results in a decrease in q_1 and q_2 values that correspond to the decreasing penetration of the jet.

The increased density of the air also increases Weber number We_{cross}, which suggests an increased tendency for liquid breakup. The extent of atomization by the high-velocity crossflow can be inferred by the expansion of the spray width with increasing downstream distance, because this expansion can only occur if the liquid jet is disintegrating. From Fig. 5, it is noted that an increase in ambient pressure leads to a progressive increase in the spread of the spray, which indicates a higher level of spray formation.

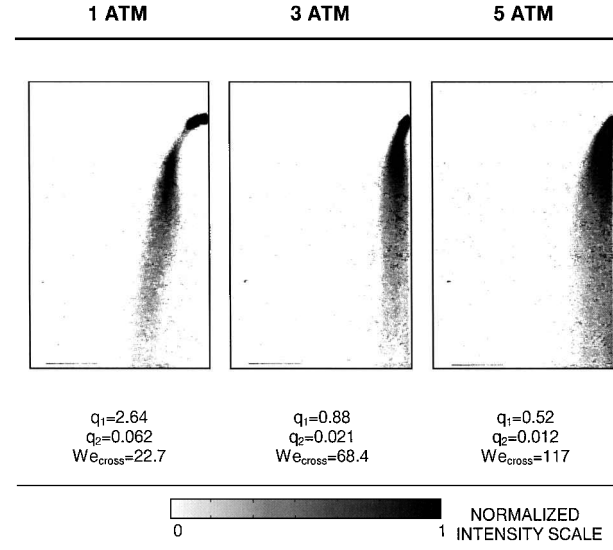

Fig. 5 Pure liquid jet injection (airblast air $\Delta P = 0\%$ and ALR = 0) under various ambient pressures.

Effect of Airblast Air at Different Ambient Pressure Conditions

The introduction of airblast air into the system increases spray atomization, as observed in Fig. 6. The images in Fig. 6 are arranged by column, according to their ambient pressure condition, and by row, according to the following atomizing air pressure drop ranges of 1.2–1.5, 2.0–2.3, and 2.9–3.3%. For the purpose of this comparison, these three groups will be referred to as the 1, 2, and 3% ranges, respectively. Each image is also labeled with its two-phase momentum-flux ratio q_2 and its ALR.

Within each ambient pressure condition, the sprays follow the expected trend of increasing jet penetration with increasing q_2. However, in comparing the sprays at each pressure condition, the spray penetration relationship to q_2 does not follow a linear function. For example, the q_2 values for the 1- and 3-atm cases at the 1 and 3% airblast ΔP conditions differ only by 0.03 and 0.01, respectively, but these differences produce a large change in the penetration of the spray. However, a larger difference in q_2 between the 3- and 5-atm sprays does not affect the jet penetration to the same degree.

The effect of introducing the airblast air can be seen by comparing the images from Fig. 5 (for $\Delta P = 0\%$) to those in the 1% ΔP range, which are presented in the first row of Fig. 6. A comparison between the $\Delta P = 0\%$ and $\Delta P = 1\%$ images does not reveal any significant increase in breakup in the regions that are downstream of and in the near field of the injection point. The jet that emerges from the injection panel is of the same dimension as the fuel orifice, which indicates that the low atomizing airflow has not led to increased instabilities leading to the breakup of the jet. The 1% atomizing air ΔP setting mainly helps to propel the liquid jet farther into the crossflow. In the 3- and 5-atm cases shown in Fig. 6, the atomizing air helps to lift the jet away from the near wall, which enhances entrainment by the crossflow and the subsequent dispersal of the spray.

As shown in Fig. 6, a continued increase in the atomizing air pressure drop results in the airblast air atomizing the liquid within the spray orifice before its injection into the crossflow. The 2% group of cases shows an expanded, atomized jet leaving the exit plane of the orifice. Increasing the airblast pressure drop to 3% yields a fully atomized spray that extends across the orifice exit, with a nodule of liquid forming at the trailing edge of the orifice.

From these observations, three distinct jet shapes occur for similar atomizing air pressure drops at the different ambient pressure cases (see Fig. 7). The first regime, which occurs for airblast pressure drops in the $\Delta P = 1\%$ range, yields an intact, discrete jet structure (Fig. 7a)

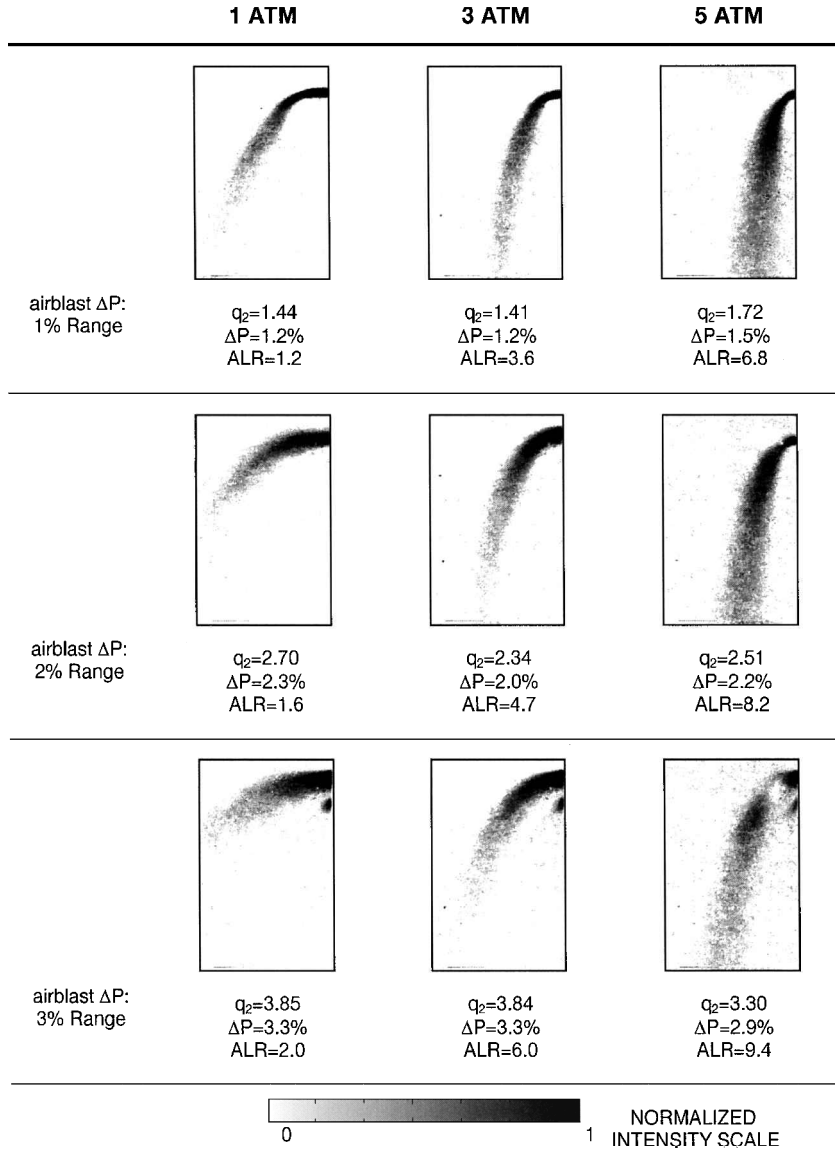

Fig. 6 Effect of atomizing air pressure drop on spray structure for various ambient pressures.

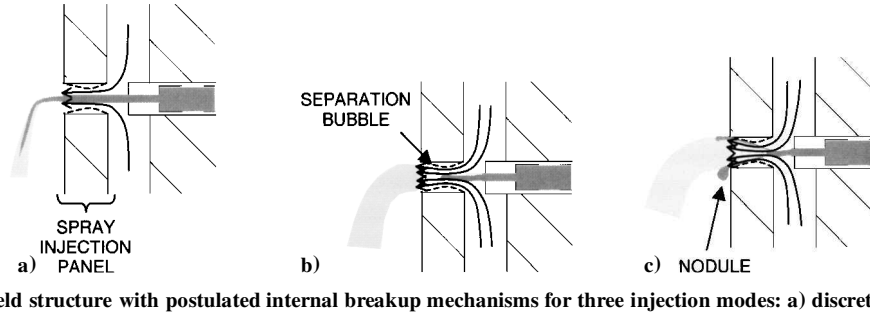

Fig. 7 Observed near-field structure with postulated internal breakup mechanisms for three injection modes: a) discrete jet, b) atomized jet, and c) fully atomized jet with a liquid nodule present.

in which the diameter of the emerging liquid jet is approximately the same as the diameter of the fuel orifice. The intact jet at the orifice exit plane is similar to the intact liquid jet for the 0% airblast ΔP case in Fig. 5. The second regime, occurring for the 2% airblast pressure drop range, forms an atomized spray across the orifice exit (Fig. 7b). The 2% airblast ΔP condition appears to be optimal in producing sprays that are well atomized and devoid of the liquid nodule that is a potential source of large droplets near the injection wall.

The third regime, which accounts for air pressure drops greater than 3%, produces a fully atomized spray across the exit plane with the appearance of a liquid nodule at the trailing edge of the jet orifice (Fig. 7c). Although the percentage of liquid contained in the nodule relative to the spray is not known, the presence of this liquid nodule may be undesirable. In Refs. 31 and 32, for example, larger droplets were observed near the injector wall in an otherwise well-atomized field of small droplets produced by airblast pressure drops above 3%. Because the spray injection panel is scaled directly to a research

fuel injector used in Ref. 33, it is possible that the nodule does form under practical combusting conditions, in which case such images of the spray structure can provide clues regarding the combustion behavior in relation to the injector.

The formation of the nodule is thought to be caused by the separation-induced internal flow pattern in the thick-walled spray orifice of the injection panel ($L_{spray}/D_{spray} = 1.4$) (see Fig. 7). An annular separation region forms as a result of the flow through the sharp-edged orifice, which results in a vena contracta that restricts the effective area of the spray orifice. Under such conditions, the lower airblast pressure drop range of 0–2% still produces atomizing air velocities that are not high enough to break up the liquid column. As the airblast pressure drop is increased, the resulting increase in the atomizing air velocities induces surface atomization and column breakup. A continued increase in the atomizing air velocity initiates atomization sooner, as the onset of atomization approaches the exit plane of the fuel injection orifice. A point is finally reached where the atomized spray interacts with the internal geometry of the spray orifice such that the fluid is concentrated toward the wall of the spray orifice. Accumulating liquid probably forms along the circumference of the spray orifice, but on injection into the crossflow, the dynamic pressure of the crossflow impacts the windward side of the spray jet and causes the pooled liquid mass to coalesce with the column of the jet. However, the pooled liquid along the leeward side of the spray jet is free from the impact of the crossflow and can, thus, form the nodule observed at the trailing edge of the orifice.

Development of a Spray Trajectory Equation

Correlations describing the jet penetration into a crossflow of air have been obtained for both gaseous (for example, Ref. 34) and liquid jets (for example, Refs. 17 and 19). Based on phenomenological considerations, the jet in crossflow correlations adhere to the following general equation, whether the centerline of gaseous jets or the upper surface of liquid jets is being described:

$$x/D_{fuel} = c_0 \times q^{c_1} \times (z/D_{fuel})^{c_2} \quad (4)$$

In this equation, c_0, c_1, and c_2 are empirically derived constants, and x/D_{fuel} and z/D_{fuel} represent the penetration and downstream distance, respectively, normalized with respect to the fuel orifice diameter D_{fuel}.

For the pure liquid jet injection cases ($\Delta P = 0\%$ and ALR $= 0$), the correlation from Ref. 19 was applied in which $c_0 = 1.37$, $c_1 = 0.50$, and $c_2 = 0.50$ (see Fig. 8). Plots depicting the outer and inner surface trajectories of the jets corresponding to the images in Fig. 5 are presented for the different ambient pressure cases. The spray boundaries are denoted by the solid dark lines, whereas the outer boundary fit of Ref. 19 is represented by the line of triangular marks overlaid on each plot. Of all of the three ambient pressure cases, the liquid jet correlation of Ref. 19 best fits the 1-atm case. The correlation fits the 3-atm case in the near-field injection region, but diverges and overpredicts jet penetration in the plane of $z/D_{fuel} = 15$. The 5-atm case, which maps only the outer surface of the jet because of the attachment of the inner surface of the jet to the wall, shows a poor fit between the correlation and the mapped outer surface. The lack of fit for the elevated pressure cases is not surprising, given that the correlation obtained in Ref. 19 was obtained under atmospheric conditions.

If the correlation of Ref. 19 were applied to the airblast-atomized spray jet, larger deviations between the correlating equation and the spray data would be produced. For a constant fuel flow rate and crossflow velocity, the value of q_1 would remain unchanged because the airblast air is not considered, and the correlating equations would yield the same results that are represented by the lines of triangles shown in Fig. 8. The airblast phase of the jet needs to be incorporated into the correlation to account for the effect of the momentum of the atomizing air on the dispersal of the spray into the crossflow. A new correlation can, thus, be obtained by applying the q_2 definition to Eq. (4).

A multivariate, nonlinear regression was performed on the data, using Eq. (4) as the basis. Equations were sought to describe the outer and inner spray boundaries, which would be useful in determining the extent of the spray at different downstream locations. The regression involved casting Eq. (4) as a linear equation through a substitution of variables and applying a least-squares fit on the resulting linear equation. The solved coefficients are then substituted back into the original equation.

The trajectory of the outer and inner surfaces of the spray for selected cases are shown in Fig. 9. The plots are arranged by column according to their ambient pressure condition. The q_2 conditions that were selected corresponded to values of q_2 approaching 0.70 (top row), 2.5 (middle row), and 5.5 (bottom row). The plots are oriented such that the spray originates from the bottom axis, with the crossflow entering from the left. The outer and inner spray surfaces are represented by the solid lines. The tracing of the spray surfaces excluded the liquid nodules that appeared in the 3% airblast ΔP cases.

Because the q_2 term is dominated by the airblast component of the spray, results from the gaseous jet correlation from Ref. 34, based on measurements of the loci of maximum velocity, are plotted to compare with the observed spray jet penetration. The gaseous jet correlation, represented by the crosshair marks, show a consistent underprediction of the spray jet penetration, that is, in a majority of the cases, below the lower surface trajectory. Although the spray jet trajectory, which is determined from the scattering of droplets in the spray, does not correlate well with the gaseous jet correlation, perhaps the atomizing air component of the spray does. It should be of interest to determine the dispersion of the atomizing air of the spray into the crossflow in further studies.

The curve fits that were derived for the outer and inner surfaces of the spray jet are also presented in Fig. 9 and are represented by

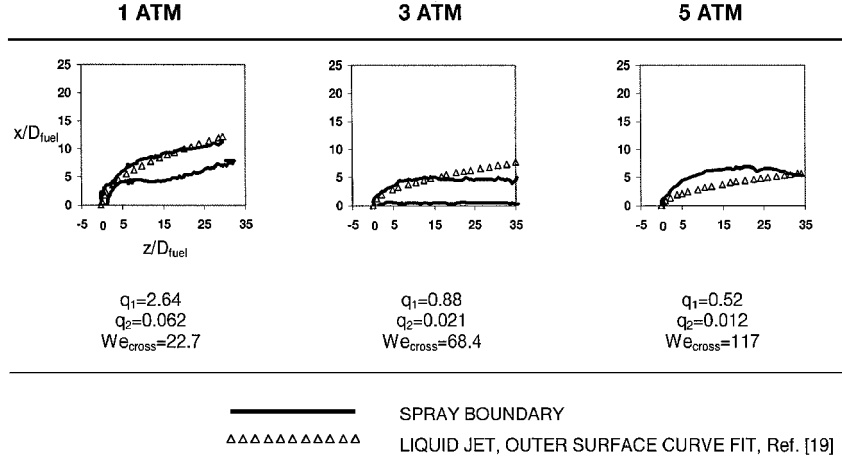

Fig. 8 Comparison of the spray surface trajectories of the pure liquid jet (airblast $\Delta P = 0\%$) obtained from the images in Fig. 5 with the outer spray surface curve fit from Ref. 19.

the triangular marks. As observed in the plots, the trajectories in the 3-atm case are well described by the curve fits. However, the curve fits underpredict the spray trajectories at the 1-atm condition and overpredict the trajectories at the 5-atm condition. One reason for the insufficient fit lies in the lack of a term to account for the atomization quality of the spray because droplets of varying sizes experience different drag forces, which would affect their trajectory. Because the ambient pressure affects the degree of atomization of the spray, one of the additional factors that was considered was a ratio of pressure normalized by a baseline pressure of $P_0 = 1$ atm. The pressure ratio was used instead of a density-related term such as a density ratio or Weber number because temperatures were not varied in this experiment. The resulting equation that was fitted in the second iteration was

$$x/D_{\text{fuel}} = c_0 \times (q_2)^{c1} \times (z/D_{\text{fuel}})^{c2} \times (P/P_0)^{c3} \qquad (5)$$

Table 1 summarizes the coefficients that describe the outer and inner surface trajectories that were derived for Eq. (5) as well as for the original curve fit in Eq. (4). In general, the power coefficients of q_2 for each of the four fitted equations are low (less than 1), but are greater than the powers of z/D_{fuel}. Whereas the power coefficients of q_2 and z/D_{fuel} are positive, the powers associated with the pressure ratio are negative. These trends make sense, given that the penetration of the spray should increase with an increase in the momentum-flux ratio and the downstream distance and should decrease with an increase in the ambient pressure.

The results of the modified curve fits are shown in Fig. 10. The spray surfaces are represented by the solid lines, whereas the triangular marks correspond to the fit with the added pressure ratio factor. The plots in Fig. 10, which are representative of the results for the other spray conditions, show that the addition of the correction factor provided a better fit to the data. The 17% average deviation of the outer edge curve fit associated with the basic trajectory correlation in Eq. (4) decreased to 7.8% for the pressure-corrected correlation in Eq. (5). For the inner spray edge, the average deviation was 69.5% for the basic trajectory correlation and 50.6% for the pressure-corrected correlation. The pressure correction improved the fit but was still deficient in predicting the inner edge of the spray, which is a region most likely populated by smaller droplets that are detrained by the crossflow from the leeside of the spray jet. For the lower edge of the spray, a factor such as the Stokes number may need to be incorporated to account for the behavior of droplets that are being entrained into the crossflow.

Table 1 Coefficients for outer and inner spray surface trajectory fits

Equation	Type	Constant c_0	Power of q_2 c_1	Power of (z/D_{fuel}) c_2	Power of (P/P_0) c_3
Basic	Outer	7.15	0.375	0.182	——
[Eq. (4)]	Inner	1.20	0.570	0.519	——
P correction	Outer	6.13	0.430	0.230	−0.336
[Eq. (5)]	Inner	0.809	0.664	0.631	−0.687

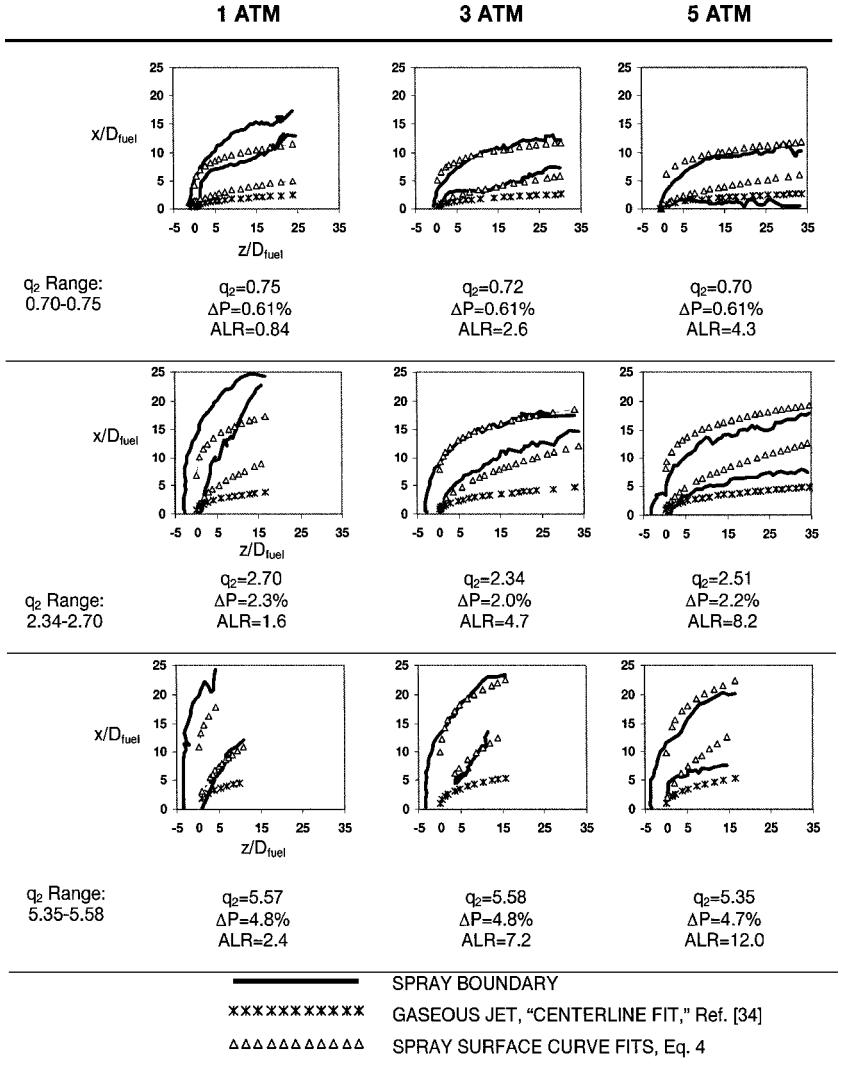

Fig. 9 Comparison of the spray surface trajectories with the gaseous jet centerline penetration correlation from Ref. 34 and the outer and inner spray surface curve fits from Eq. (4) for selected cases.

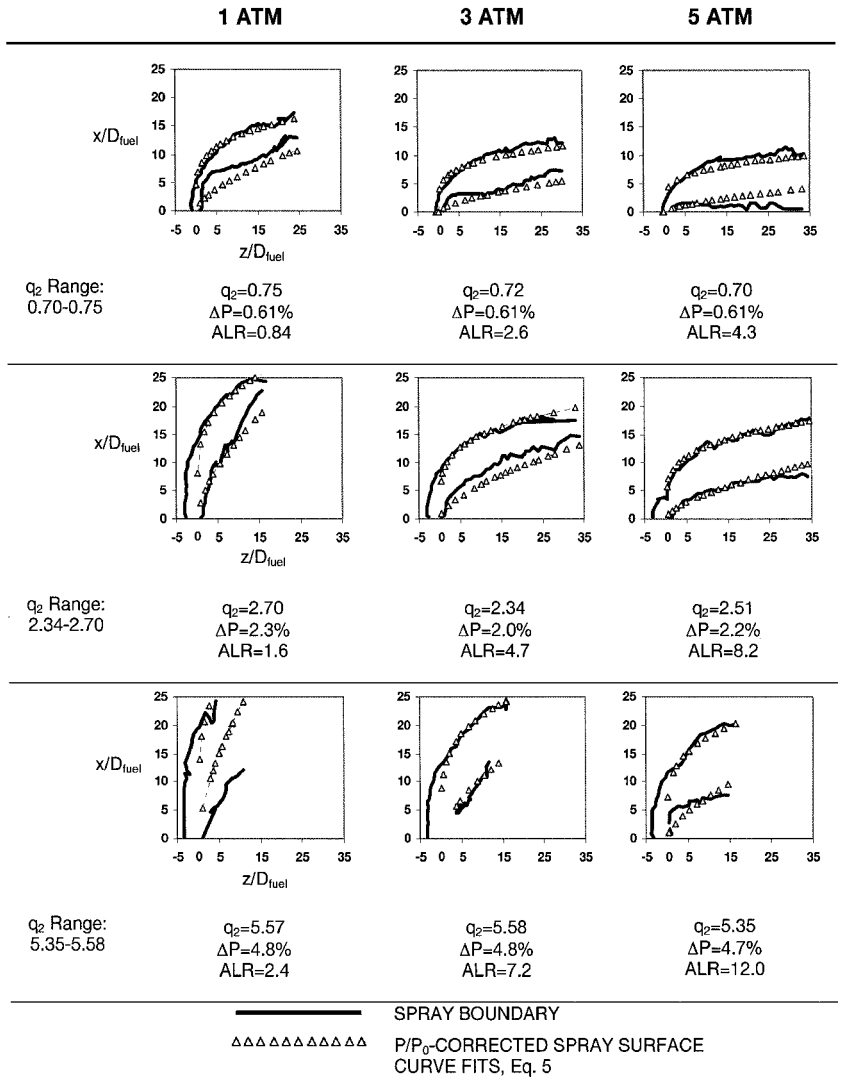

Fig. 10 Comparison between the spray surface trajectories and the pressure-term corrected curve fits from Eq. (5) for selected cases.

The spray trajectory correlations that were obtained are valid for the operating and geometric conditions of the present study. These operating conditions correspond to a low-power operating regime in a gas turbine engine. Note that additional data are required at other conditions (e.g., at varying fuel mass flow rates, additional crossflow velocity magnitudes, and different spray orifice diameters) to provide a complete variation of the q_2 parameter for equation fitting. Nonetheless, the ability to fit an equation to spray jets using a bulk parameter such as q_2 at various ambient pressure conditions is encouraging, especially given that varying degrees of atomization are obtained at the different conditions.

Conclusions

Spray scattering images were used to investigate the structure of the airblast-atomized spray jet injected into a crossflow of air under varying ambient pressure conditions. At each ambient pressure, the airblast airflow rate was varied to yield airblast pressure drops ranging from 0 to 4.8% across the injector orifice. The crossflow velocity magnitude centered on a baseline value of 38 m/s. For the airblast-atomized liquid jet injected into a crossflow of air and under varying ambient pressures of 1, 3, and 5 atm, the following conclusions were found:

1) At a given jet-to-crossflow momentum-flux ratio in which the airblast pressure drop, fuel flow rate, and crossflow velocity are held constant, an increase in ambient pressure decreases spray jet penetration and increases breakup.

2) Across the range of ambient pressures tested, an increase in the atomizing air pressure drop, which increases the velocity of the atomizing air, results in an increase in spray jet penetration and breakup. Three modes of spray structure occur at the point of injection under different atomizing air operating regimes, independent of the ambient pressure: a) discrete jet ($0 < \Delta P < 2\%$), b) atomized jet ($2\% < \Delta P < 3\%$), and c) fully atomized jet with a liquid nodule at the trailing edge ($\Delta P > 3\%$).

4) A jet penetration equation of the form

$$(x/D_{\text{fuel}}) = c_0 \times q^{c_1} \times (z/D_{\text{fuel}})^{c_2}$$

can be used to describe both outer and inner surface trajectories of the spray jet, if the following definition of the two-phase jet to crossflow momentum-flux ratio q_2 is used:

$$q_2 = \frac{\left[(\rho V^2 A)_{\text{liquid}} + (\rho V^2 A)_{\text{airbl}}\right] / A_{\text{spray}}}{(\rho V^2)_{\text{cross}}}$$

However, the added complexities of atomization and momentum transfer associated with the airblast flow produce spray trajectories that are better described if the penetration equation is corrected with a pressure ratio term P/P_0.

Acknowledgments

This research program was supported by the NASA John H. Glenn Research Center at Lewis Field under Contract NCC3-412, with J. D. Holdeman and R. R. Tacina serving as Contract Monitors. The authors also thank R. L. Hack, S. W. Lee, F. Akamatsu, and J. Moon for their assistance in the setup of the experiment and in the

collection and processing of data. F. Akamatsu was supported by Kobe University and participated in this work while spending one year at the University of California, Irvine Combustion Laboratory.

References

[1]Lyons, V. J., "Fuel/Air Nonuniformity: Effect on Nitric Oxide Emissions," *AIAA Journal*, Vol. 20, No. 5, 1981, pp. 660–665.

[2]Zelina, J., and Ballal, D. R., "Combustor Stability and Emissions Research Using a Well-Stirred Reactor," *Journal of Engineering for Gas Turbines and Power*, Vol. 119, No. 1, 1997, pp. 70–75.

[3]Fric, T. F., "Effects of Fuel-Air Unmixedness on NO_X Emissions," *Journal of Propulsion and Power*, Vol. 9, No. 5, 1993, pp. 708–713.

[4]Adelberg, M., "Breakup Rate and Penetration of a Liquid Jet in a Gas Stream," *AIAA Journal*, Vol. 5, No. 8, 1967, pp. 1408–1415.

[5]Heister, S. D., Nguyen, T. T., and Karagozian, A.R., "Modeling of Liquid Jets Injected Transversely into a Supersonic Crossflow," *AIAA Journal*, Vol. 27, No. 12, 1989, pp. 1727–1734.

[6]Inamura, T., "Trajectory of a Liquid Jet Traversing Subsonic Airstreams," *Journal of Propulsion and Power*, Vol. 16, No. 1, 2000, pp. 155–157.

[7]Inamura, T., and Nagai, N., "Spray Characteristics of Liquid Jet Traversing Subsonic Airstreams," *Journal of Propulsion and Power*, Vol. 13, No. 2, 1997, pp. 250–256.

[8]Inamura, T., Nagai, N., Watanabe, T., and Yatsuyanagi, N., "Disintegration of Liquid and Slurry Jets Traversing Subsonic Airstreams," *Experimental Heat Transfer, Fluid Mechanics and Thermodynamics*, edited by M. D. Kelleher et al., Elsevier, Amsterdam, New York, 1993, pp. 1522–1529.

[9]Kihm, K. D., Lyn, G. M., and Son, S. Y., "Atomization of Cross-Injecting Sprays into Convective Air Stream," *Atomization and Sprays*, Vol. 5, Nos. 4–5, 1995, pp. 417–433.

[10]Kitamura, Y., and Takahashi, T., "Stability of a Liquid Jet in Air Flow Normal to the Jet Axis," *Journal of Chemical Engineering of Japan*, Vol. 9, No. 4, 1976, pp. 282–286.

[11]Less, D. M., and Schetz, J. A., "Transient Behavior of Liquid Jets Injected Normal to a High-Velocity Gas Stream," *AIAA Journal*, Vol. 24, No. 12, 1986, pp. 1979–1986.

[12]Li, H.S., and Karagozian, A. R., "Breakup of a Liquid Jet in Supersonic Crossflow," *AIAA Journal*, Vol. 30, No. 7, 1992, pp. 1919–1921.

[13]Mazallon, J., Dai, Z., and Faeth, G. M., "Primary Breakup of Nonturbulent Round Liquid Jets in Gas Crossflows," *Atomization and Sprays*, Vol. 9, No. 3, 1999, pp. 291–311.

[14]Nejad, A. S., and Schetz, J. A., "Effects of Properties and Location in the Plume on Droplet Diameter for Injection in a Supersonic Stream," *AIAA Journal*, Vol. 21, No. 7, 1983, pp. 956–961.

[15]Nguyen, T. T., and Karagozian, A. R., "Liquid Fuel Jet in Subsonic Crossflow," *Journal of Propulsion and Power*, Vol. 8, No. 1, 1992, pp. 21–29.

[16]Oda, T., Hiroyasu, H., Arai, M., and Nishida, K., "Characterization of Liquid Jet Atomization Across a High-Speed Airstream," *JSME International Journal, Series B*, Vol. 37, No. 4, 1994, pp. 937–944.

[17]Schetz, J. A., and Padhye, A., "Penetration and Breakup of Liquids in Subsonic Airstreams," *AIAA Journal*, Vol. 15, No. 10, 1977, pp. 1385–1390.

[18]Thomas, R. H., and Schetz, J. A., "Distributions Across the Plume of Transverse Liquid and Slurry Jets in Supersonic Airflow," *AIAA Journal*, Vol. 23, No. 12, 1985, pp. 1892–1901.

[19]Wu, P. K., Kirkendall, K. A., Fuller, R. P., and Nejad, A. S., "Breakup Processes of Liquid Jets in Subsonic Crossflow," *Journal of Propulsion and Power*, Vol. 13, No. 1, 1997, pp. 64–73.

[20]Wu, P. K., Kirkendall, K. A., Fuller, R. P., and Nejad, A. S., "Spray Structures of Liquid Jets Atomized in Subsonic Crossflows," *Journal of Propulsion and Power*, Vol. 14, No. 2, 1998, pp. 173–182.

[21]Ghosh, S., and Hunt, J. C. R., "Spray Jets in a Cross-Flow," *Journal of Fluid Mechanics*, Vol. 365, 1998, pp. 109–136.

[22]Holterman, H. J., van de Zande, J. C., Porskamp, H. A. J., and Huijsmans, J. F. M., "Modelling Spray Drift from Boom Sprayers," *Computers and Electronics in Agriculture*, Vol. 19, No. 1, 1997, pp. 1–22.

[23]Phillips, J. C., and Miller, P. C. H., "Field and Wind Tunnel Measurements of the Airborne Spray Volume Downwind of Single Flat-Fan Nozzles," *Journal of Agricultural Engineering Research*, Vol. 72, No. 2, 1999, pp. 161–170.

[24]Phillips, J. C., Miller, P. C. H., and Thomas, N. H., "Air Flow and Droplet Motions Produced by the Interaction of Flat-Fan Sprays and Cross Flows," *Atomization and Sprays*, Vol. 10, No. 1, 2000, pp. 83–103.

[25]Lefebvre, A. H., *Atomization and Sprays*, Hemisphere, Washington, DC, 1989.

[26]Edelman, R. B., Economos, C., and Boccio, J., "Mixing and Combustion in Two-Phase Flows with Application to the B–O–H–N System," *AIAA Journal*, Vol. 9, No. 10, 1971, pp. 1935–1940.

[27]Han, K. S., and Chung, M. K., "Numerical Simulation of Two-Phase Gas–Particle Jet in a Crossflow," *Aerosol Science and Technology*, Vol. 16, No. 2, 1992, pp. 126–139.

[28]Salzman, R. N., and Schwartz, S. H., "Experimental Study of a Solid–Gas Jet Issuing into a Transverse Stream," *Journal of Fluids Engineering*, Vol. 100, No. 3, 1978, pp. 333–339.

[29]Chin, J. S., Freeman, W. G., and Lefebvre, A. H., "Evaporation Histories of Fuel Sprays Injected Across a Flowing Air Stream," *Atomization and Spray Technology*, Vol. 2, No. 2, 1986, pp. 135–149.

[30]Crowe, C. T., Sharma, M. P., and Stock, D. E., "The Particle-Source-in Cell (PSI-Cell) Model for Gas–Droplet Flows," *Journal of Fluids Engineering*, Vol. 99, No. 2, 1977, pp. 325–332.

[31]Seay, J. E., McDonell, V. G., and Samuelsen, G. S., "Atomization and Dispersion from a Radial Airblast Injector in a Subsonic Crossflow," AIAA Paper 95-3001, July 1995.

[32]Leong, M. Y., McDonell, V. G., and Samuelsen, G. S., "Cross-Sectional Spray Patternation of an Airblast-Atomized Liquid Jet Injected into a Crossflow," *Proceedings of the 7th International Conference on Liquid Atomization and Spray Systems*, Seoul, South Korea, Aug. 1997, pp. 294–301.

[33]Shaffar, S. W., and Samuelsen, G. S., "A Liquid Fueled, Lean Burn, Gas Turbine Combustor Injector," *Combustion Science and Technology*, Vol. 139, Nos. 1–6, 1998, pp. 41–57.

[34]Kamotani, Y., and Greber, I., "Experiments on a Turbulent Jet in a Crossflow," *AIAA Journal*, Vol. 10, No. 11, 1972, pp. 1425–1429.

[35]Holdeman, J. D., "Mixing of Multiple Jets with a Confined Subsonic Crossflow," *Progress in Energy and Combustion Science*, Vol. 19, No. 1, 1993, pp. 31–70; see also NASA TM 104412, 1991.